



Numerical analysis of a standard wind turbine blade using ANSYS Fluent

Shreyas Kotian

Department of Mechanical and Aerospace Engineering, University of California- San Diego, San Diego, CA, 92093, USA

ABSTRACT

With the natural sources of the world fast depleting, it is time that we find alternate sources of energy. There are various alternatives such as solar energy, hydroelectric, geothermal energy, wind energy, and nuclear energy. Wind energy has gained popularity in current times with an increase in energy production from 6 billion kWh in 2000 to 434 billion kWh in the US as per the U.S Energy Information Administration. A significant part in the extraction of maximum energy from the wind turbine is to understand the aerodynamics of wind turbine blades and improve their design. The current study focuses on the computational analysis of various aerodynamic parameters around the wind blade using ANSYS Fluent. The results obtained from the study are presented in this paper

Key words: Turbine blade, ANSYS Fluent, Numerical simulation

1. INTRODUCTION

Wind power is really coming to the forefront as a means of energy production with non- renewable sources of energy like coal, gas, and petroleum fast depleting [1]. Being inexhaustible, it is the fastest growing technology in the world. By the end of 2011, China was able to install about 63 GW capacity of wind turbines [2]. An important component of the wind turbine which plays a major role in the energy of wind production is the design of the blades of the wind turbine. As they are the devices which rotate which further creates energy, having an accurate shape is paramount. Along with the shape, the structural and material properties of the wind blade also play an important role in determining the efficiency of the wind turbine. As known by previous knowledge, that theoretically it is only possible to harness 59.2% of the incoming energy of the moving wind, attempts are being made to reach as close as possible to it.

The aim of the present study is to numerically analyze, the flow around a wind blade, the torque and power generated by the blade, and the velocity and pressure field across the blade with the given geometry. More details about the analysis are presented in the following sections.

2. GEOMETRY

The geometry of the given blade has been developed in SOLIDWORKS and further analysis like, developing the flow domain, creating named selections has been done in Space claim and numerical analysis has been done in ANSYS FLUENT. A 3D view of the wind blade is shown in Fig. 1, Fig. 2 shows a cut section of the wind blade which tells us about the aero foil used in the blade

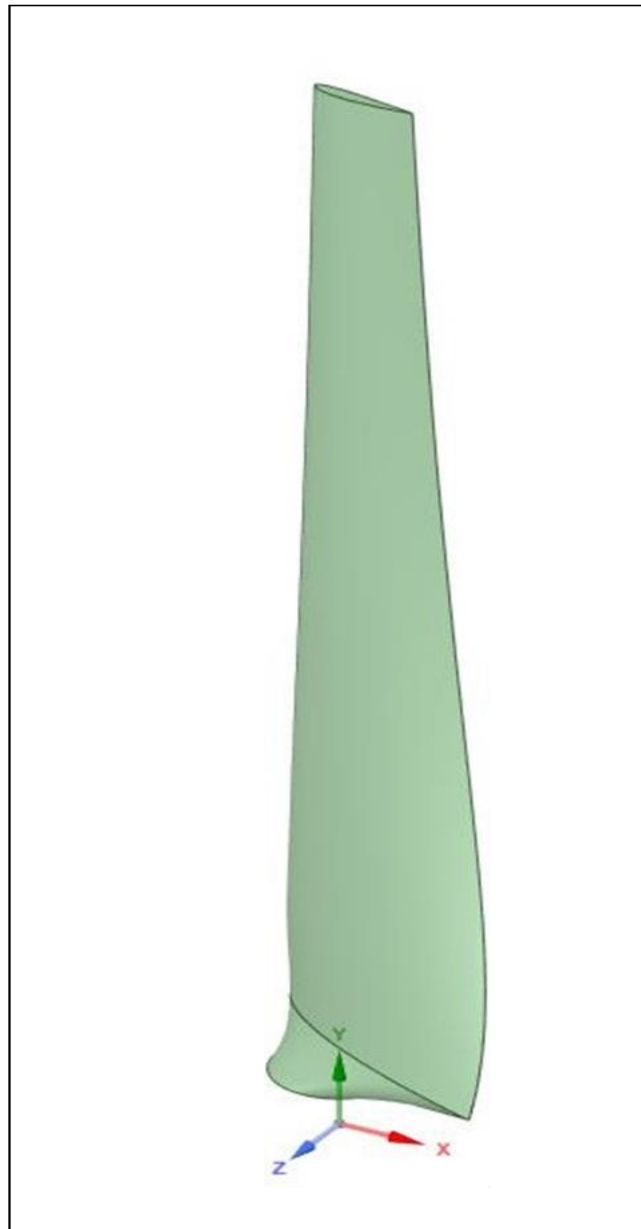


Figure 1: dimensional view of the blade.

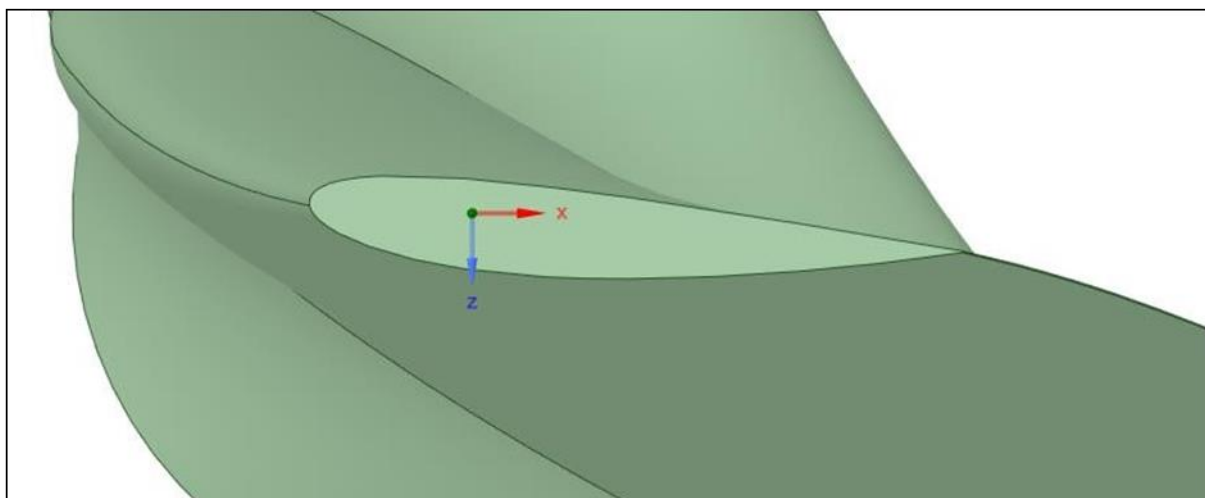


Figure 2: Cut section of the blade showing the airfoil.

3. COMPUTATIONAL METHODOLOGY

3.1. Numerical Solution

The numerical solution for the given problem is solved by the finite volume method. Once the geometry has been created, and meshing has been done, which divided the whole fluid domain into small cells or control volumes. Once this has been established ANSYS FLUENT would solve each of the parameters such as x, y, and z velocity, energy, turbulent kinetic energy (k), and specific rate of dissipation present in the differential equations which govern them such as continuity, velocity, and momentum. This gives us the value of the parameters at the center of the control volume. Then with the help of interpolation, values at other locations are determined.

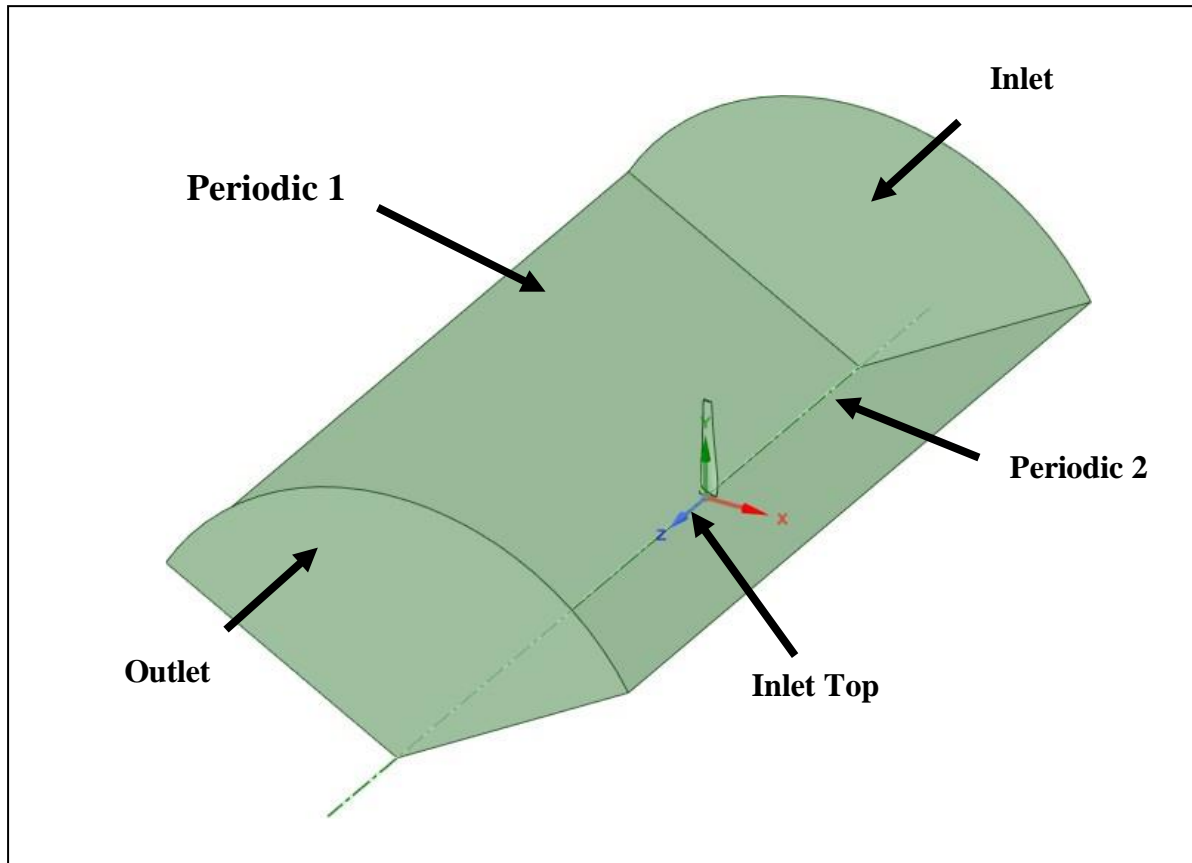


Figure 3: Computational domain of the blade.

3.2. Mathematical Model and Flow Domain Extents

In the current investigation, the geometry of the model was displayed utilizing SOLIDWORKS and meshing was finished utilizing ANSYS FLUENT with Meshing 2021 R1. As the three blades of the wind turbine are symmetric, one blade is analyzed in the fluid domain to decrease the computational cost. The length of the wind blade is approximately 305 mm with an offset of 40 mm given at the root of the wind blade to accommodate the rotor and hub. To develop the fluid domain, an arc with an angle of 120° was drawn which is pulled 2.5 times the wind blade length in the negative z direction and 5 times the wind blade length in the positive z direction which encloses the fluid domain in which analysis has to be done.

After the following has been done, each of the individual surfaces are given named selections such as inlet, outlet, inlet top, periodic 1, and periodic 2 as shown in Fig. 3 so that it is easier for one to specify the boundary conditions in FLUENT.

3.3. Mesh Topology

The ANSYS FLUENT with meshing tool was being used to mesh the data. For the simulations, face size meshing was done on the blade wall, as it is the region of our interest in our analysis. A surface mesh was also created with a minimum size of 0.0021 mm and a maximum size of 0.05625 mm. The growth rate is set to 1.2 with curvature and proximity on. Periodic boundary conditions are set up and boundary layers are added and finally the whole volume is meshed. The above meshing gives about 29,703 nodes and 10,389 faces. Fig. 4

shows the view of the meshed domain. Fig. 5 shows the close up view of the blade and Fig. 6 shows the close up view of the blade near the airfoil.

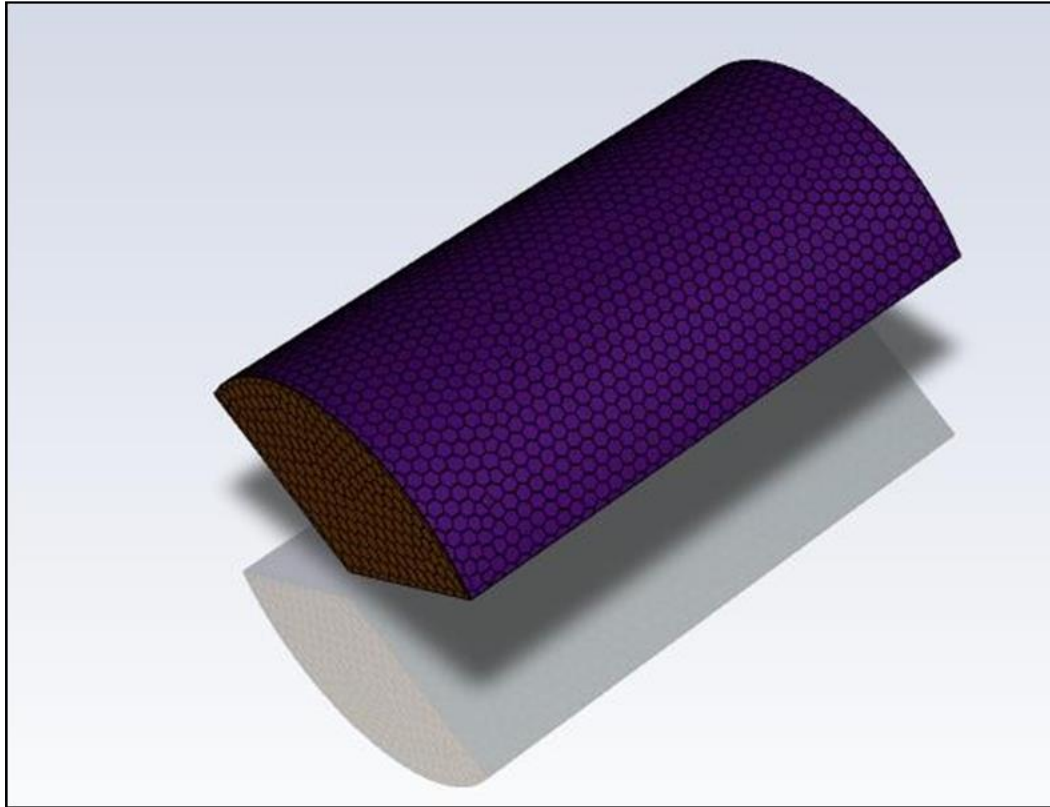


Figure 4: Final mesh of the blade.

Turbine Blade

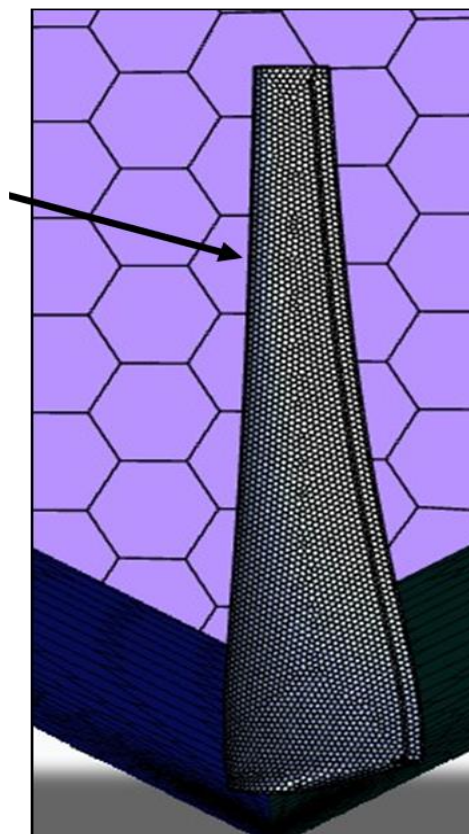


Figure 5: Close-up view of the mesh of the blade

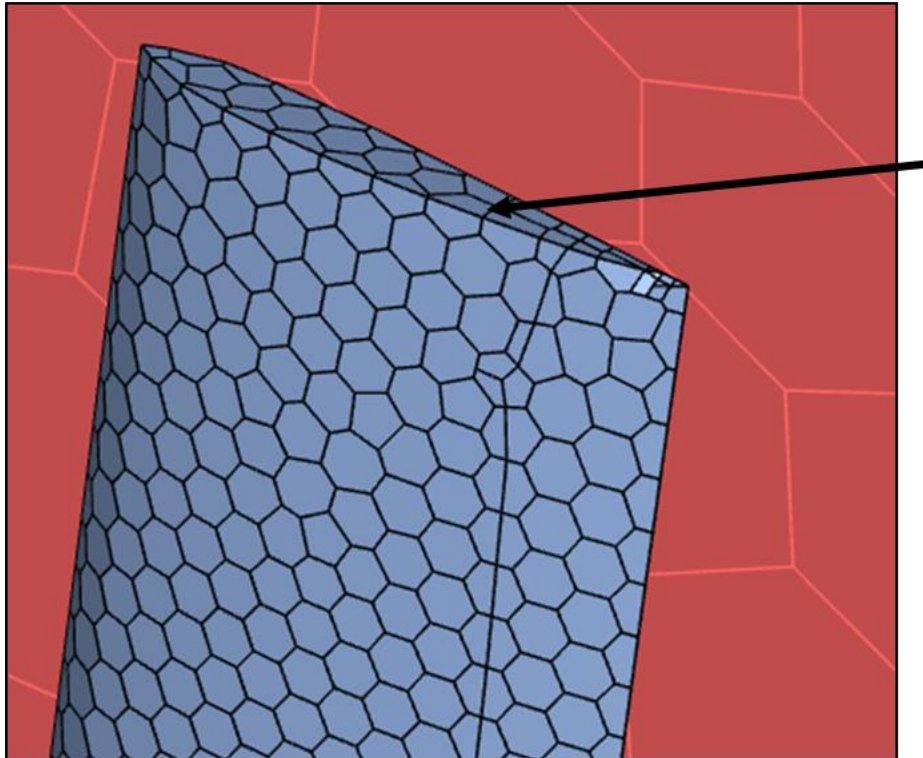


Figure 6: Close-up view of the mesh at the edge of the blade

3.4. Boundary Conditions

As shown in Fig. 3 there are five named selections namely inlet, inlet_top, outlet, periodic 1 and periodic 2. Different boundary conditions are given for the same as mentioned in Table 1. Periodic 1 and Periodic 2 are set as periodic boundary conditions and they have no specified value.

Table 1: Boundary conditions for the given problem.

Named Selection	Boundary Condition	Magnitude
Inlet	Velocity Inlet	6 m/s
Inlet_Top	Velocity Inlet	6 m/s
Outlet	Pressure Outlet	101,325 Pa

3.5. Model Setup and Solution

Once the turbulence model has been selected which in this case is the $k-\omega$ model, we proceed further with the set up. In materials the we select fluid as air with a density of 1.225 kg/m^3 and a dynamic viscosity of 1.7894×10^{-5} as per standard conditions. As the wind turbine is rotating, we select a rotating frame of reference from the axis of rotation $\{0,0,0\}$ to $\{0,0,1\}$. The angular speed of the turbine is set to 98 rad/s . We set the residual to 0.001 as anything greater than that would take a lot of computational time. Under initialization we set the conditions to standard and compute from the inlet. Iterations are set to 1500 and the solution runs till the convergence criteria is not met.

4. RESULTS AND DISCUSSION

The following section presents a summary of the results which include pressure distribution across the blade, velocity, and pressure profiles at different locations along the length of the windblade and the effect of tip speed ratio and pitch angle of the power of the wind blade.

Fig. 7 shows a plot of the pressure integral. As we can observe the pressure remain almost constant and is equivalent to the atmospheric pressure.

Fig. 8 shows the residuals converging. Repeated spikes can be observed after 1000 iterations as the solution was run for different tip speed ratios.

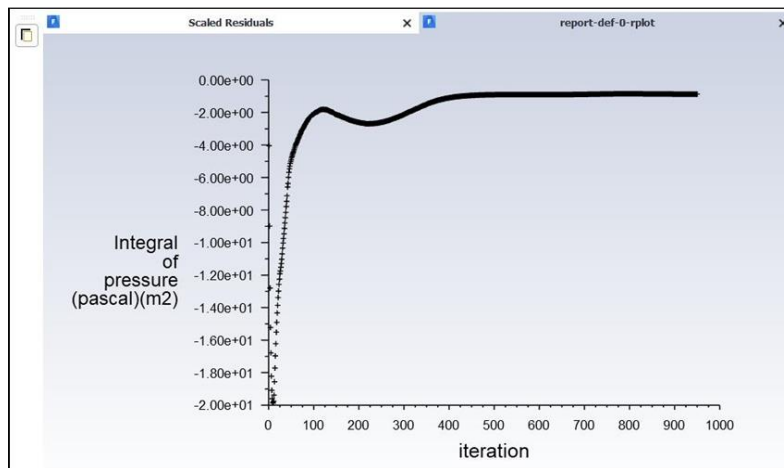


Figure 7: Plot of pressure integral

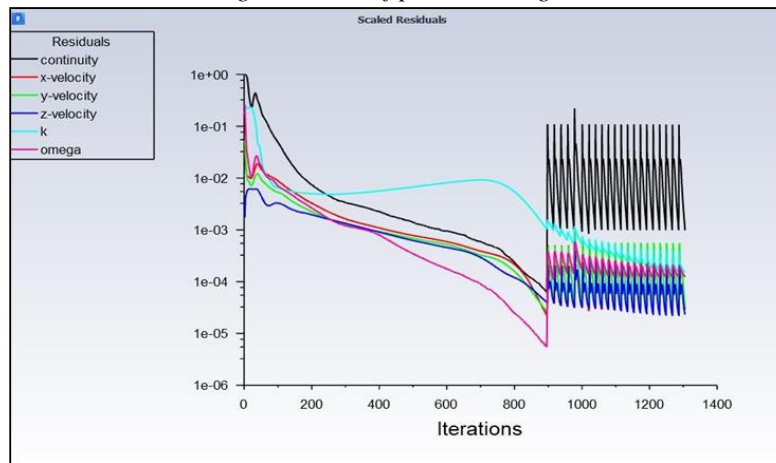


Figure 8: Plot of the converged solution.

4.1. Pressure Distribution across different sides of the wind blade

The following section presents the results of pressure distribution of the windward and leeward side of the wind blade for a pitch angle of 4°. As expected on the windward side (Fig. 9). The pressure is quite less which translates that the velocity of fluid across it would be greater in accordance with Bernoulli’s principle. Hence, the contours are accurate and meet our expectations.

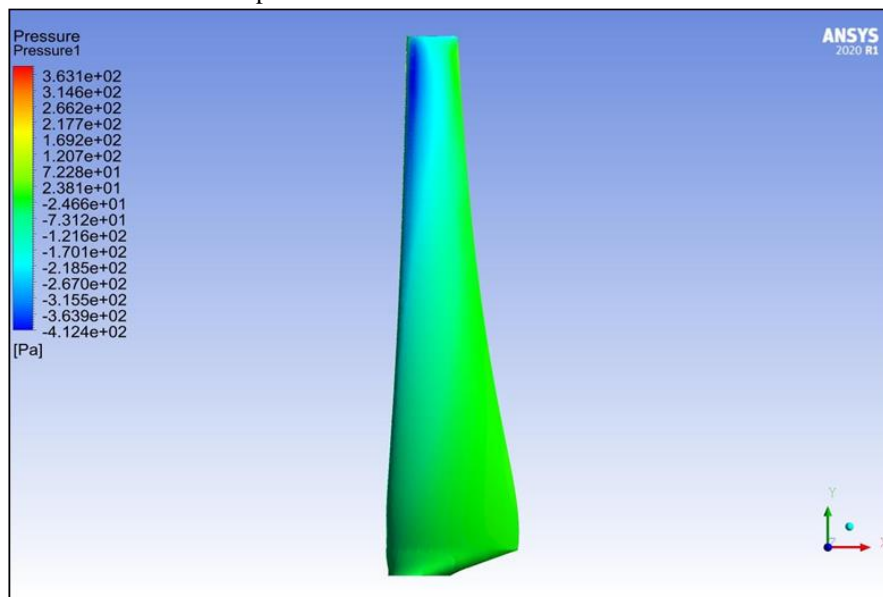


Figure 9: Pressure distribution across the blade on the windward side

The leeward side (Fig. 10) shows a higher-pressure distribution along the blade which results in the velocity being lower on that surface which is again in accordance to Bernoulli’s principle.

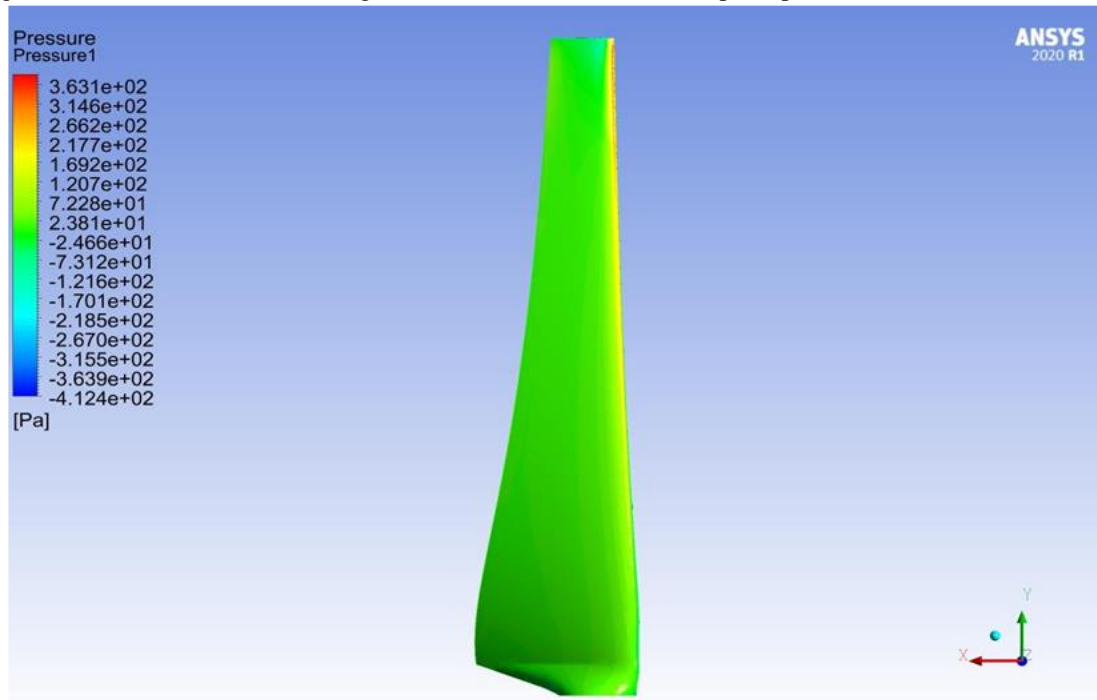


Figure 10: Pressure distribution across the blade on the leeward side

4.2. Pressure and Velocity Distribution at different locations along the length of the blade

The following section presents pressure and velocity distributions along different planes along the length of the blade. For convenience, three different locations have been assumed. One, just at the root of the blade, which is at a distance of 0.055 m, one at the middle at 0.1775 m, and one at the top at 0.3m.

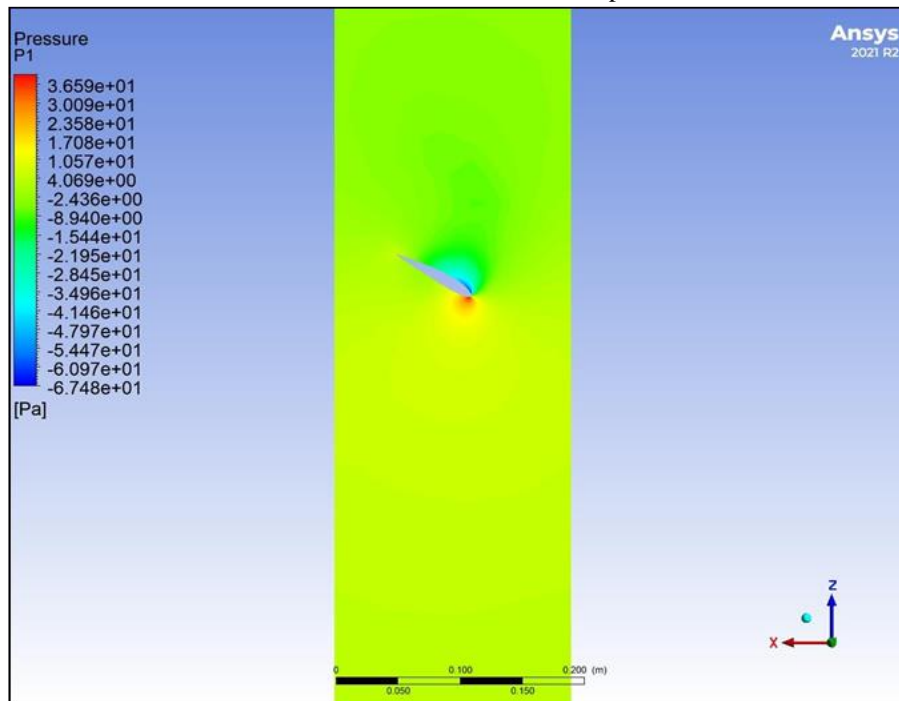


Figure 11: Pressure distribution across the blade at 0.055 m

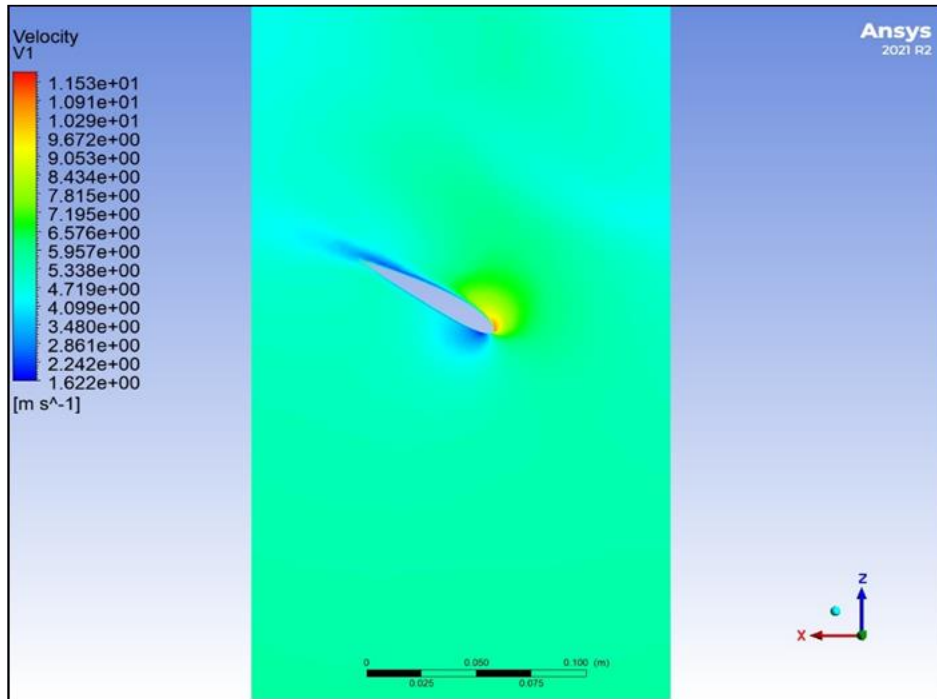


Figure 12: Velocity distribution across the blade at 0.055 m

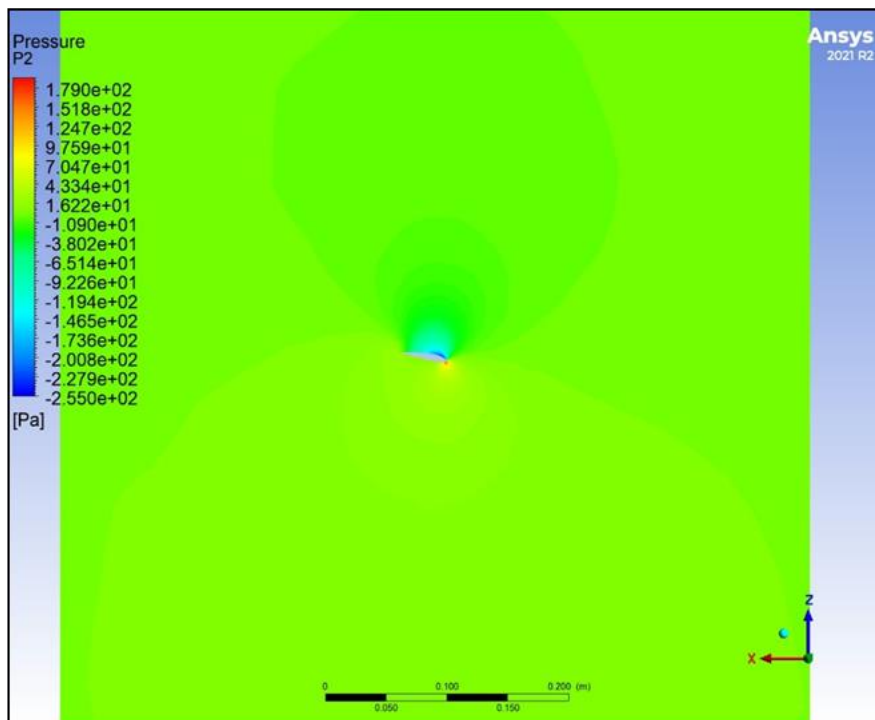


Figure 13: Pressure distribution across the blade at 0.1775 m

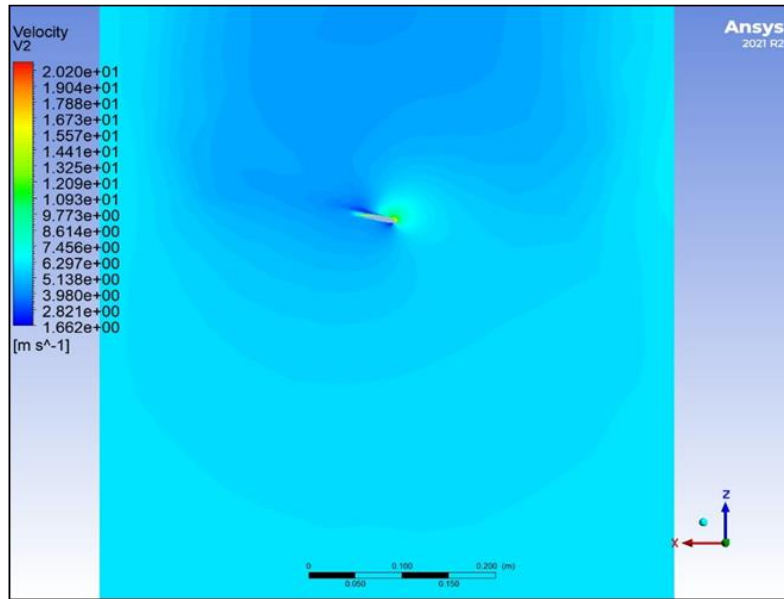


Figure 14: Velocity distribution across the blade at 0.1775 m

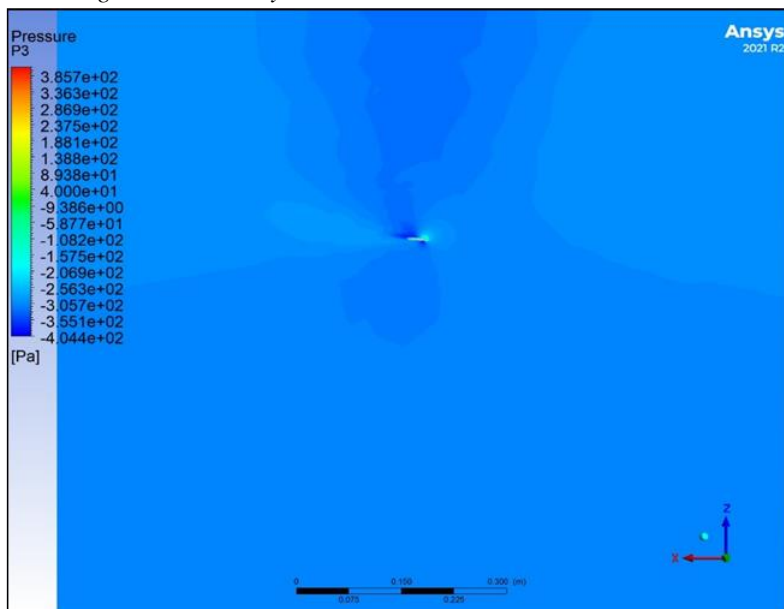


Figure 15: Pressure distribution across the blade at 0.3 m.

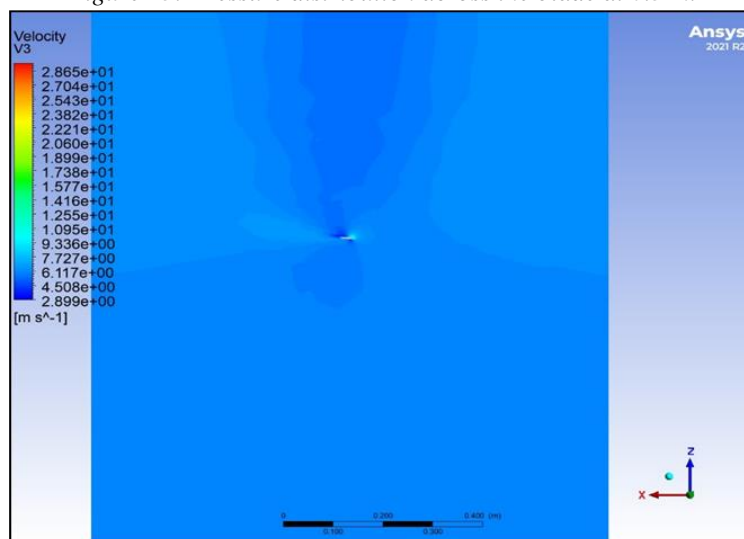


Figure 16: Velocity distribution across the blade at 0.3 m

Through the pressure contours at various locations (Fig. 11, Fig. 13, Fig. 15), we can see that as we move away from the blade, the magnitude of the pressure keeps decreasing which is also true because maximum velocity is achieved at the tip of the blade. Maximum velocity results in minimum pressure according to Bernoulli's theorem. At the lower side of the airfoil, we distinctly observe a red region and a blue region on the top of the airfoil. According to the legend the magnitude of pressure on the lower side is higher than that on the upper side which results in the production of lift.

An opposite trend is observed in the velocity contours (Fig. 12, Fig. 14, Fig. 16). Higher velocity is observed on the upper surface of the airfoil and lower velocity on the lower surface of the airfoil which is in accordance with our expectations.

Pressure decreases as we move away from the blade which causes the velocity to increase. This shows that the maximum velocity is produced at the tip of the blade. Practically, 1/3rd from the tip of the blade is where the maximum power is produced.

4.3 Effect of tip speed ratio and pitch angle on the power produced by the wind blade.

The following section presents the effect of pitch angle on the performance parameters of the wind blade.

Table 2: Performance parameters of the wind blade for a pitch angle of 4°

Pitch angle of 4°					
Tip Speed Ratio (λ)	Rotational velocity (ω)	Torque (N-m)	Power (W)	Power Coefficient	
4		78.689	0.0268	6.327	0.164
	4.2	82.623	0.0284	7.039	0.182
	4.4	86.557	0.03027	7.860	0.203
	4.6	90.492	0.03146	8.541	0.221
	4.8	94.426	0.03233	9.158	0.237
5		98.361	0.0328	9.679	0.250
	5.2	102.295	0.03328	10.213	0.264
	5.4	106.230	0.0335	10.676	0.276
	5.6	110.164	0.0331	10.939	0.283
	5.8	114.098	0.0324	11.090	0.287
6		118.033	0.0313	11.083	0.287
	6.2	121.967	0.03	10.977	0.284
	6.4	125.902	0.0284	10.727	0.277
	6.6	129.836	0.0265	10.322	0.267
	6.8	133.770	0.0246	9.872	0.255
7		137.705	0.0226	9.336	0.241
	7.2	141.639	0.0204	8.668	0.224
	7.4	145.574	0.0181	7.905	0.204
	7.6	149.508	0.0158	7.087	0.183
	7.8	153.443	0.0134	6.168	0.160
8		157.377	0.011	5.193	0.134
8.2		161.311	0.0087	4.210	0.109
8.4		165.246	0.00624	3.093	0.080

Table 3: Performance parameters of the wind blade for a pitch angle of 2°

Pitch angle of 2°					
Tip Speed Ratio (λ)	Rotational velocity (ω)	Torque (N-m)	Power (W)	Power Coefficient	
4		78.689	0.0311	7.342	0.190
	4.2	82.623	0.032	7.932	0.205
	4.4	86.557	0.033	8.569	0.222
	4.6	90.492	0.0342	9.284	0.240
	4.8	94.426	0.0352	9.971	0.258
	5	98.361	0.0363	10.711	0.277
	5.2	102.295	0.0374	11.478	0.297
	5.4	106.230	0.038	12.110	0.313
	5.6	110.164	0.038	12.559	0.325
	5.8	114.098	0.0374	12.802	0.331
	6	118.033	0.0385	13.633	0.353
	6.2	121.967	0.035	12.807	0.331

6.4	125.902	0.0334	12.615	0.326
6.6	129.836	0.0312	12.153	0.314
6.8	133.770	0.0288	11.558	0.299
7	137.705	0.0263	10.865	0.281
7.2	141.639	0.0236	10.028	0.259
7.4	145.574	0.0208	9.084	0.235
7.6	149.508	0.018	8.073	0.209
7.8	153.443	0.015	6.905	0.179
8	157.377	0.0181	8.546	0.221
8.2	161.311	0.012	5.807	0.150
8.4	165.246	0.0057	2.826	0.073

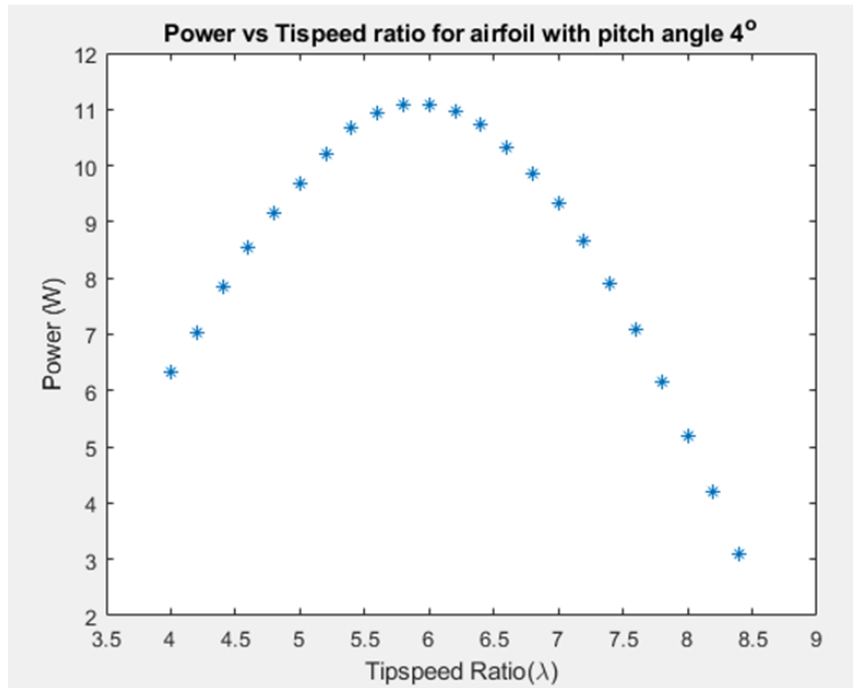


Figure 17: Effect of tip speed ratio on power of the blade with a pitch angle of 4°.

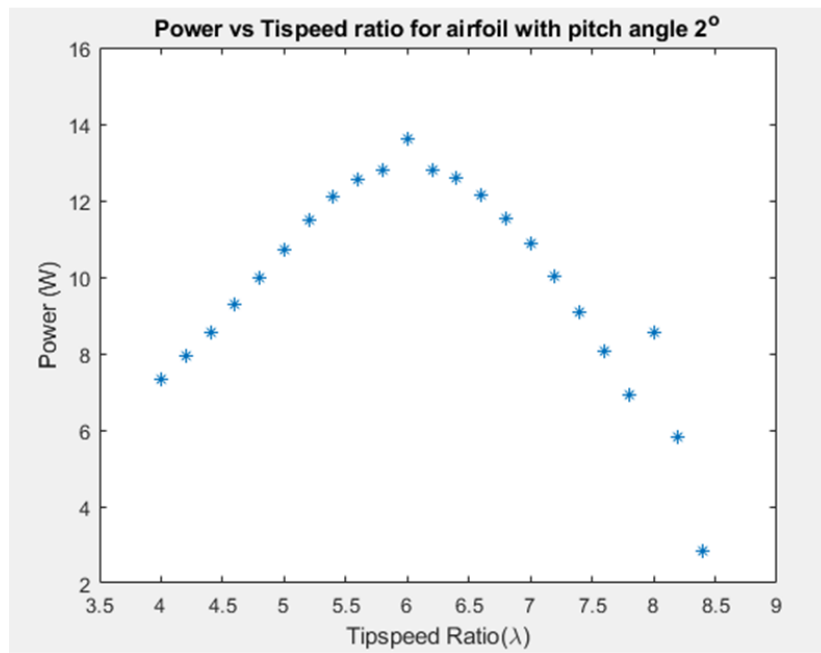


Figure 18: Effect of tip speed ratio on power of the blade with a pitch angle of 2°.

Through the following graphs (Fig. 18, Fig. 19) we can observe that irrespective of the pitch angle of the airfoil, power produced by the wind turbine blade increases as tip speed ratio increases, reaches a maximum limit, and then starts to decrease. This is in accordance with Betz's Law.

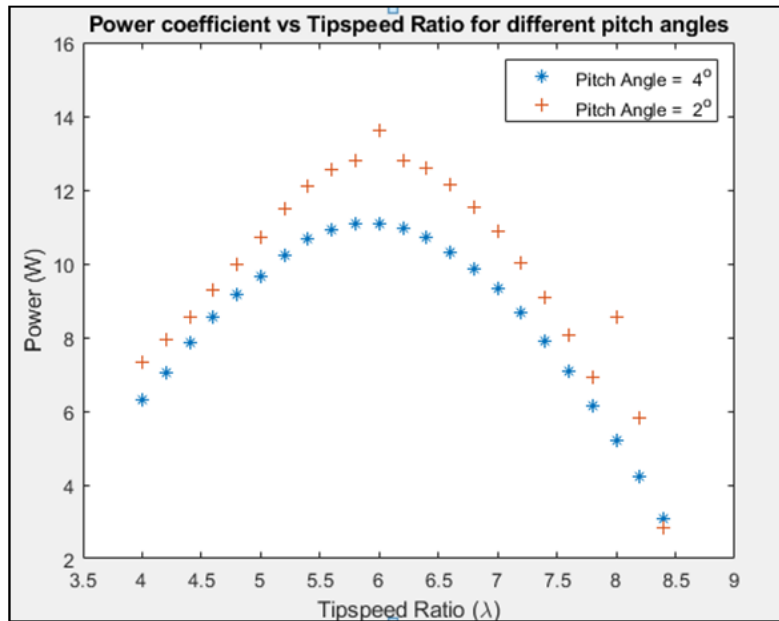


Figure 19: Effect of tip speed ratio on power of the blade with varying pitch angles of the airfoil

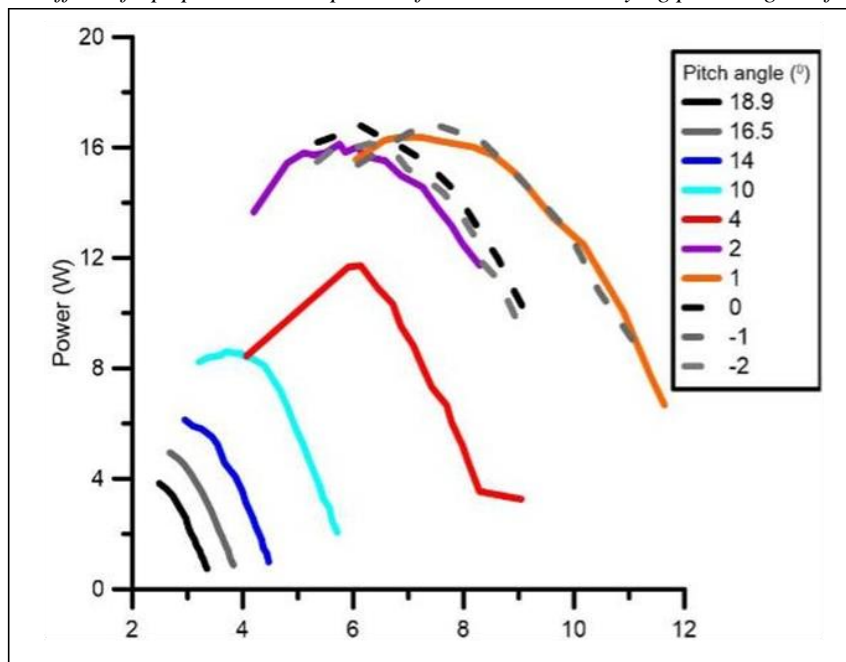


Figure 20: Experimental data of effect of tip speed ratio on power of the blade with varying pitch angles of the airfoil

Through Fig. 20, we observe that at the same tip speed ratio, an airfoil with pitch angle of 2° produces more lift than a 4° airfoil. When we compare the following results to the experimental data (Fig. 21) they are in good accordance. For the wind blade with pitch angle of 4° , maximum power is obtained at tip speed ratio of 6 which is also the case from our computational results. For blade with pitch angle of 2° , the peak flattens out between tip speed ratio of 6 and 7 and from our numerical analysis, the tip speed ratio comes out at 6. So, the results are in good agreement. Fig. 22 shows a comparison of the two airfoils with the Betz limit. As we can observe, the wind turbine is not able to extract maximum power from the incoming wind and the aerodynamic performance of the wind turbine can be improved. The power coefficient seems reasonable as it follows the Betz law and for all tip speed ratio's the value is less than 0.59 (Betz Limit).

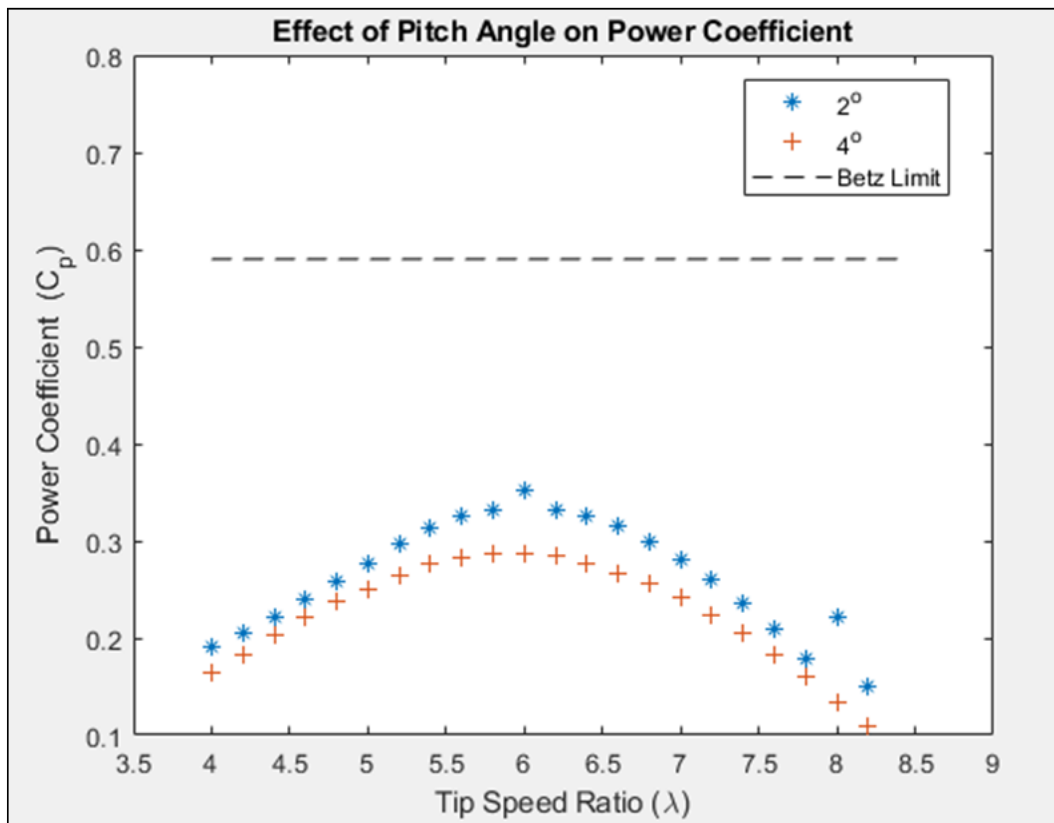


Figure 21: Effect of tip speed ratio on power coefficient of the blade with varying pitch angles of the airfoil

5. CONCLUSIONS AND FUTURE WORK

The present study focuses on the computational analysis of the aerodynamic performance of a wind turbine. A wind blade with varying pitch angles have been investigated and a summary of the results are presented in this section.

- From the pressure contours it was observed that the pressure on the leeward side was greater than the pressure on the windward side.
- Pressure decreases as we move away from the blade which causes the velocity to increase. This shows that the maximum velocity is produced at the tip of the blade. Ideally, $1/3^{\text{rd}}$ from the tip of the blade is where the maximum power is produced.
- Irrespective of the pitch angle of the blade, the power produced increases with tip speed ratio, reaches a maximum and then decreases.
- A blade with a pitch angle of 2° produces more power than a blade with pitch angle of 4° at a particular value of tip speed ratio.

Based on the analysis it can be observed that the wind blade isn't able to extract maximum performance (Fig. 21), so a consideration would be to improve the design of the wind blade so that maximum output can be achieved.

REFERENCES

- [1]. Sayed, M., Kandil, H., and Shaltot, A., 2012, "Aerodynamic analysis of different wind turbine blade profiles using finite-volume method," *Energy Conversion and Management*, 64, pp. 541- 550.
- [2]. Wang, T., 2012, "A brief review of wind turbine dynamics," *Theoretical and Applied Mechanics Letters*, 2, 062001.
- [3]. Manwell, J.F., McGowan, J.G., Rogers, A.L., *Wind Energy Explained- Theory, Design and Application* (pp. 21-82), John Wiley & Sons Ltd, 2002.